Ecological Indicators 144 (2022) 109548

Contents lists available at ScienceDirect

Ecological Indicators

journal homepage: www.elsevier.com/locate/ecolind

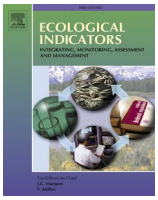

Original Articles

A GIS-based multicriteria decision analysis to reduce riparian vegetation hydrogeological risk and to quantify harvested biomass (Giant reed) for energetic retrieval

L. Sciuto [a,*], F. Licciardello [b], A.C. Barbera [b], G. Cirelli [b]

[a] International Doctorate in Agricultural, Food and Environmental Science – Di3A – University of Catania, Italy
[b] Dipartimento di Agricoltura, Alimentazione e Ambiente (Di3A), Università degli Studi di Catania, Via S. Sofia, 100, Catania 95123, Italy

ARTICLE INFO

Keywords:
Arundo donax L.
Riparian vegetation management
Hydraulic risk
Invasive species
Remote sensing
Biochemical methane potential

ABSTRACT

The vegetation development in riverbeds creates obstructions to the regular water flow with the flooding hydraulic risk increase. Giant reed (GR) (*Arundo donax* L.) is one of the most successful invasive species of riparian ecosystems in Mediterranean semi-arid climate conditions, with significant public administrations costs for its removal and disposal. At the meantime, due to its high biomass yield and adaption capacity to several conditions, GR is a very promising no-food crop to produce biogas by the anaerobic digestion (AD). The research activity provides for the involvement of territories belonging to the inner areas of Sicily, especially Calatino one, in which the SIMBIOSI Consortium operates an AD plant fed with agricultural by-products from other close agro-industrial companies. The aim of the study was to map and to quantify the actual spatial distribution of GR in watercourses embankments through Remote Sensing (RS) techniques applied in a Geographic Information System (GIS) environment. In this regard, a method based on the automatic supervised classification, was applied on three different combinations of spectral bands (True Color Image – TCI; Near-Infrared, Green and Blue – NGB; Vegetation Red Edge – VRE) of Sentinel-2 satellite images related to the summer season (11th August 2019), with the aim of identifying the most suitable classification to map the GR. The results showed that the VRE composition is the most accurate combination of spectral bands for the identification of GR, followed by the NGB image. The worst performance was obtained by using the TCI combination. A further elaboration was carried out combining the three classified images, in order to obtain a more accurate localization and quantification of GR. The final thematic map allowed to correctly classify GR for the 46 % of the cases, with an overall accuracy of 85.02 % and a high Kappa Coefficient of Agreement value equal to 0.81. Finally, the surface covered by GR in the study area (computed in the GIS environment) was about 2 km^2 and the estimated GR biomass, available for the biomethane production, obtainable from watercourses embankments maintenance interventions would amount to about 11,780 tons $year^{-1}$. The study could contribute to the development of a watercourses maintenance plan with the aim to reduce the risk of streams flooding in valley areas and at intersections with infrastructure works. Furthermore, the proposed methodology can be used by stakeholders in marginal areas, for the watercourses management, offsetting its costs through the energy use of the collected biomass.

1. Introduction

According to the Water Framework Directive (WFD) (2000/60/EC) the protection and the enhancement of water bodies ecological status is of paramount importance for promoting sustainable water use (Carvalho et al., 2019; Todo & Sato, 2002). Its main objective is to achieve a good status of all aquatic ecosystems, surface water and groundwater bodies, respecting certain standards for the ecological, chemical and biological quality of waters. The European Environment Agency (EEA) reported that the quantity and quality of about 60 % of surface water bodies, due to many pressures, were failing to reach a good ecological status (European Environment Agency, 2018). The river basin management is an appropriate instrument to reduce pressures on European freshwater integrating and balancing environmental, social and economic changes. In this sense, in 2009, some progress has been reached with the 1st River Basin Management Plans (RBMPs). However, the improvements have

* Corresponding author.
E-mail address: liviana.sciuto@phd.unict.it (L. Sciuto).

https://doi.org/10.1016/j.ecolind.2022.109548
Received 26 July 2022; Received in revised form 28 September 2022; Accepted 5 October 2022
Available online 11 October 2022

been not accomplished with the original expectations. For this reason, the 2nd RBMPs which will cover the 2016–2021 period includes new measures able to achieve the Directive's objective readily. Additionally, there is an increasing recognition that measures undertaken in river basin management should offer multiple advantages, across sectors. To this end, the European Commission has already started to evaluate the WFD through a "Fitness check" on the Water Framework Directive and the Floods Directive (European Commission, 2017). An evaluation process on the "Blueprint to Safeguard Europe's Water Resources" also taken place (European Commission, 2012), highlighting the need for a marked improvement and an increased integration of WFD goals into other policy areas, such as the Common Agriculture Policy (CAP), the Cohesion and Structural funds and the policies on renewable energy, and transport and integrated management of floods and droughts.

Within this framework, riparian vegetation plays a multifunctional role in different hydraulic, sedimentological and ecological processes reducing erosion, stabilizing stream banks, controlling water quality and enriching the habitat and aesthetic values of the streams (Forzieri, 2012; Lama et al., 2021a; Meixner et al., 2006; Naiman et al., 1993). Unfortunately, the vegetation development in riverbeds creates reduction of flow velocity aggravating floods hydraulic risk (Li et al., 2022; Recchia et al., 2010). As a consequence, it is important to plan the correct management and maintenance interventions to reduce hydrogeological risk, especially in urban areas in which extreme precipitation events have severe impacts due to land use change and population growth (Mahmood et al., 2017). In many cases the costs of cutting and removing the vegetation are unsustainable, and the disposal of biomass is a significant burden with the economic resources of public administrations. Therefore, it is necessary to evaluate the possibility of reusing biomass from the mowing of watercourses embankments for energy purpose, in order to recover at least a part of vegetation management costs and to create new economic opportunities in the floodplain areas for energy production (Forzieri, 2012; Recchia et al., 2010; Rockwood et al., 2004).

In this regards, giant reed (GR) is one of the most successful invasive species of riparian ecosystem in semi-arid climate conditions, enough to be included in a list of the 100 World's worst alien species (Lowe et al., 2000; Pilu et al., 2013). It is considered a hydrophyte plant capable to alter the natural drainage of channel causing the risk of streams flooding (Jiménez-Ruiz et al., 2021; Spencer et al., 2013). Despite it shows the traits of invasive plant species, GR has aroused the interest of the scientific community for its best potential in the EROEI value (Energy Returned On Energy Invested) in comparison with other energy crops (Pilu et al., 2012; Pilu et al., 2013). This is due to its great adaptability to different pedoclimatic conditions in combination with the high biomass yield and the low input required for its growth (Borin et al., 2013; Corno et al., 2014; Pilu et al., 2013). Numerous studies reported that in semi-arid climate conditions the GR average production ranges between 21 and 51 t ha^{-1} (Angelini et al., 2009; Antal, 2018; Barbagallo et al., 2013; Barbagallo et al., 2014; Borin et al., 2013; Mantineo et al., 2009). According to several authors, taking into account the positive traits, GR could be considered a very promising no-food crop to produce biogas by the anaerobic digestion (AD) (Barney & DiTomaso, 2008; Corno et al., 2014; Crosti et al., 2010; Ge et al., 2016; Pilu et al., 2013).

The literature reports numerous case studies, all over the world, where Geographic Information System (GIS) based methodologies combined with statistical data are used to quantify and to localize biomasses for energy purpose, including agricultural and harvesting residues, industrial waste and by-products from industrial production and processes (Cai et al., 2008; Kumar et al., 2015; Pantaleo et al., 2013; Roberts et al., 2015; Valenti et al., 2018a; Yanli et al., 2010). However, a limited number of studies used Remote Sensing (RS) techniques integrated with GIS tools to detect in an automatic way the spatial distribution of the riparian vegetation with the aim to quantify its availability for biogas and biomethane productions. For instance, Dillabaugh & King (2008) performed a classification process employing Ikonos multispectral and panchromatic images to identify the riparian marshland composition and the biomass along the Rideau River in eastern Ontario. Forzieri et al. (2010) applied a supervised pixel-based approach to detect and to monitor the riparian vegetation over a 14-km stretch of the Sieve River using both QuickBird images and LIDAR data (Light Detection and Ranging). Also, Everitt et al. (2008) used QuickBird and SPOT 5 multispectral satellite images to map GR along the Rio Grande River near Del Rio in southwest Texas. In recent times, Lama et al. (2021b) studied the riparian vegetation impacts on flow resistance mapping the presence of aquatic vegetation (*Arundo donax* L.) along an abandoned drainage channel located in Nola (Campania, Southern Italy) by using multispectral images acquired through Unmanned Aerial Vehicles (UAV), in order to estimate the bulk drag coefficient on the basis of Leaf Area Index (LAI) map derived by an Normalized Difference Vegetation Index (NDVI) assessment.

On this basis, the aim of this work is focused on the enhancement and sustainable reuse of the biomass from watercourses embankments for bioenergy production by the AD, in order to mitigate the risk of streams flooding and to support maintenance interventions costs given the lack of a supply chain (80–100 € per tons, personal information). The main novelty of this study is represented by the integration of the environmental and economic advantages of GR harvesting, especially in the inner areas of Sicily characterized by heightened phenomena of climate changes causing water scarcity, droughts and flood hydraulic risk increases, typical of the Mediterranean environment mostly in the last decades. Particularly the studied area (Calatino) is often subjected to floods due to the wide distribution of GR along the watercourses embankments. However, the significant availability of by-products from the close agro-industrial companies and the presence of a biogas plant to reuse in a sustainable way residues from harvesting, recovering the management vegetation costs, and to reduce some environmental impacts could become a real opportunity for this territory. As reported by Kumar Khanal et al. (2021), in fact, one of the key factors for the bioconversion of feedstock is the microbial community chosen for the initially inoculation of reactors essential for starting the AD process. Biogas plants are supplied with various types of inoculum from agricultural residues with multiple and active microorganism, which affect the digestion process performance (Alavi-Borazjani et al., 2020; Kumar Khanal et al., 2021; Valenti et al., 2018b).

Specifically, the objective of this study was addressed by mapping the actual spatial distribution of GR along watercourses embankments, through Geographic Information System (GIS) environment using the Remote Sensing (RS)-based classification algorithm, with the aim to quantify the amount of GR available for both biogas and biomethane production. Compared to the previous studies, we introduced a new approach based on the combination of different spectral band compositions in order to improve the accuracy of the final GR mapping.

2. Materials and methods

2.1. Study area

The research was carried out in the inner area of Sicily "Calatino" (Italy); it covers eight Sicilian municipalities (Caltagirone, Grammichele, Licodia Eubea, Mineo, Mirabella Imbaccari, San Cono, San Michele di Ganzaria and Vizzini) belonging to the Catania province. The activity was conducted in collaboration with SIMBIOSI Consortium, that operates, within the municipality of Mineo, an AD plant fed with agricultural by-products from other close agro-industrial companies. Biomass samples for the quantification of GR yield were harvested in an area along the Caltagirone riverbanks (Fig. 1).

The stream, with a length of 26.47 km, rises in close proximity to the Caltagirone municipality and flows into the Monaci river, that is the main right bank tributary of the Gornalunga river, which in turn is one of the main watershed of Simeto river. The Caltagirone watershed has an area of 199.64 km^2 (at the junction with the Ferro river, pouring into the Monaci river) and a perimeter of 100.63 km, with an elevation ranging

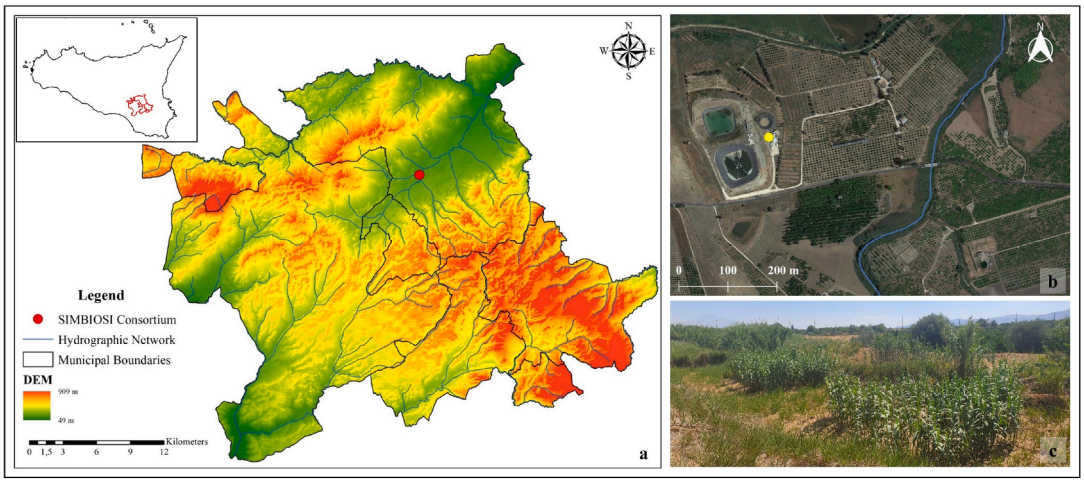

Fig. 1. (a) Calatino area, with the boundaries of the involved municipalities, and SIMBIOSI Consortium in the red circle; (b) company area and localization of anaerobic digestion plant in the yellow circle; (c) embankements of the Caltagirone river. (For interpretation of the references to color in this figure legend, the reader is referred to the web version of this article.)

from 90.07 to 688.27 m above the sea level; the mean elevation is 321.50 m and the mean basin slope is 14.67 % (Fig. 2).

Table 1 summarizes the main morphometric characteristics of the Caltagirone watershed basin, resulting from a spatial analysis performed using a Digital Elevation Model (DEM) with 20×20 m resolution in the GIS environment.

The Calatino territory is located in a semi-arid climate area characterized by climate changes causing extreme precipitation events with flood hydraulic risk increases, especially in the last few years. The territory is equipped with several weather stations managed since 2002 by the SIAS (Sicilian Agrometeorological Information Service), able to record different variables, including rainfall, temperature and humidity. In order to compute the area of influence of each weather stations, a GIS-based spatial analysis was performed to identify the one that provides an adequate spatial coverage of the area under study. In particular, the Thiessen polygons method, also known as Voronoi polygons, was used to assign an areal significance to weather variables recorded as point values (Fig. 3).

The spatial analysis showed that the Caltagirone weather station polygon cover a larger area of the Caltagirone watershed with respect to the Mineo weather station, providing a spatial coverage of about 124,01 km^2 corresponding to 62.12 % of the whole basin area. Considering the location of the study area falling within the Caltagirone weather station zone of influence and the upstream position of the latter with respect to the biomass harvested site, the meteorological data recorded by this station were taken into account for the elaboration of this study. Moreover, the Caltagirone weather station recorded higher rainfall depth than the one of Mineo (based on the data recorded during the period 2002–2021) with a mean annual rainfall of about 675.43 mm and

Table 1
Morphometric characteristics of Caltagirone catchment.

Parameters	Value
Area (km^2)	199.64
Perimeter (km)	100.63
Main pathway length (km)	26.47
Maximum altitude (m)	688.27
Minimum altitude (m)	90.07
Mean altitude (m)	321.50
Altitude difference (m)	598.20
Main pathway slope (%)	2.26
Mean basin slope (%)	14.67

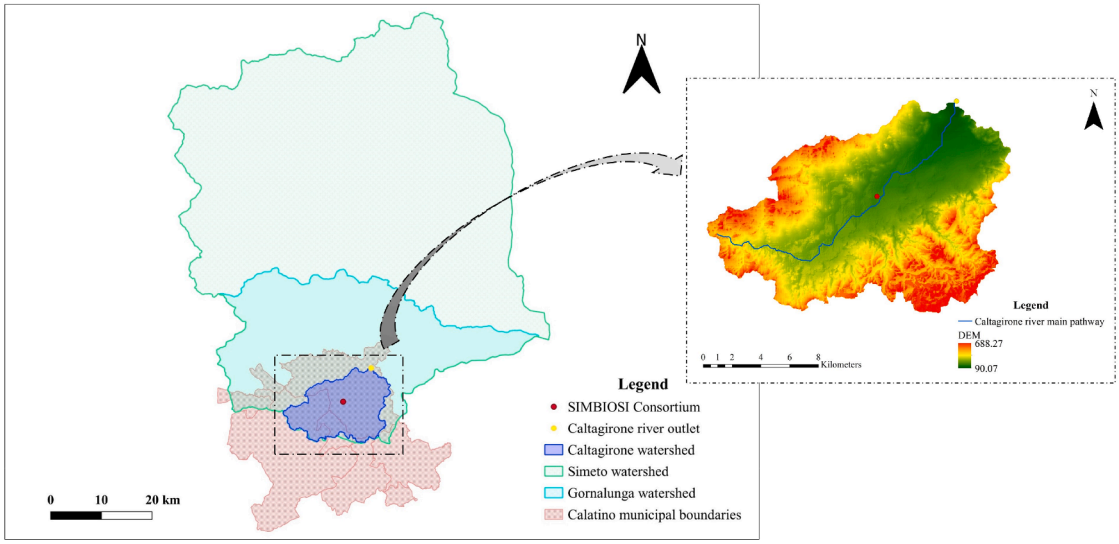

Fig. 2. Location of the Caltagirone catchment in the inner area of Calatino (Eastern Sicily, Italy).

613 mm respectively in the two stations, allowing to consider the worst case scenario. As regard the temperature, the discussed time span was characterized by a mean annual temperature of 17 °C, ranging from a minimum of 8.19 °C up to a maximum of 26.90 °C, with a relative humidity of 38.67 %. Meteorological data, including mean annual rainfall and temperature, recorded by the weather station located in the territory of Caltagirone are reported in Fig. 4.

Numerous rainfall events occurred in the Calatino area, in the last year, although not all of extreme intensity caused significant phenomena of flooding hydraulic in valley areas and at intersections with infrastructure works. The main cause was the uncontrolled vegetation development in river beds and its inadequate management at the hands of the public administration (i.e. basin authority, consortium of reclamation), resulting in a significant reduction of the hydraulic section and river floods.

The precipitation event occurred on the 11th November 2021 caused the Caltagirone river flood with severe damages to access routes, infrastructures and cultivated fields. In Fig. 5 are illustrated the rainfall probability curves for return periods of 2, 5, 10, 20, 50 and 100 years of the Caltagirone pluviographic station related to the data recorded from 1930 to 2015 and the event occurred last November. The graph in Fig. 5 shows that this is not a significant event, considering that only for a three hours' duration ranks near the return period of 2 years; in all other cases is always below establishing itself as a more frequent rainfall event.

2.2. A GIS-based analysis to assess the spatial distribution of Arundo donax L

The methodology carried out to identify and to quantify the surface covered by giant reed (GR), was based on the integrated use of Remote Sensing (RS) techniques and Territorial Information System (SIT) (able to easily process satellite data and to extract information about an object or a phenomenon of the real world) (Shanmugapriya et al., 2019).The principle behind RS is the possibility to discriminate the Earth's features, such as soil, vegetation and water, by the radiometric behavior that distinguishes them. In this regard, a method of "pattern recognition", based on the automatic supervised classification, was applied on three different combinations of spectral bands (True Color Image – TCI; Near-Infrared, Green and Blue – NGB; Vegetation Red Edge – VRE) of Sentinel-2 satellite images (Table 2) related to the summer season (11th August 2019), with the aim of identifying the most suitable classification to map the GR.

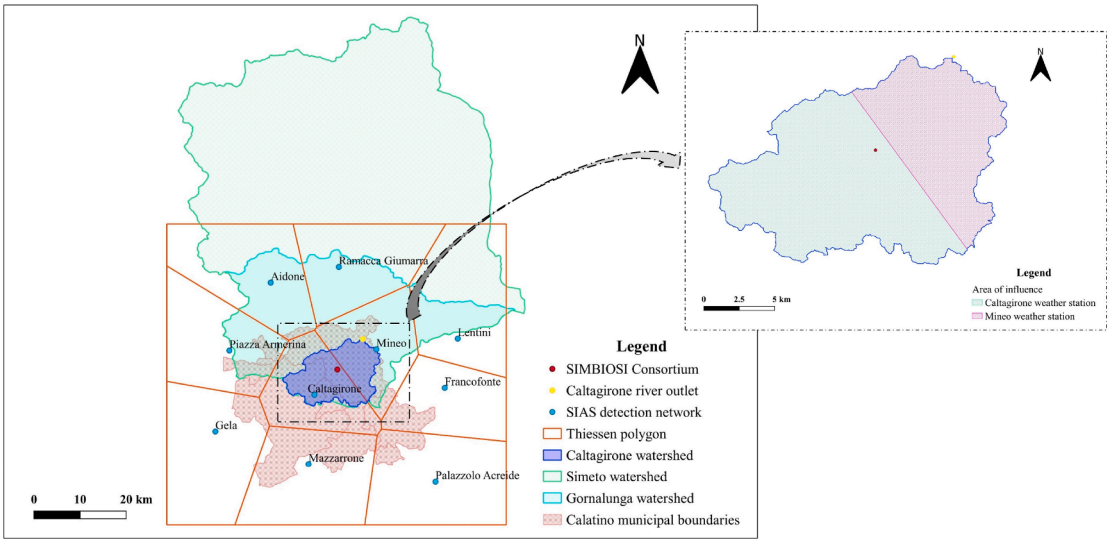

Fig. 3. Polygons method identified by the thiessen method in the study area.

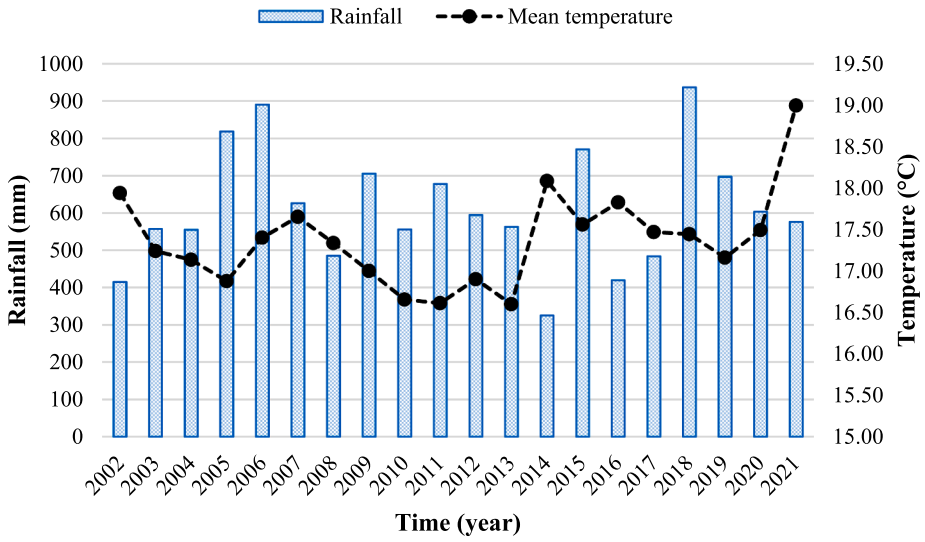

Fig. 4. Meteorological data, mean annual rainfall and temperature, recorded by the Caltagirone weather station (2002–2021).

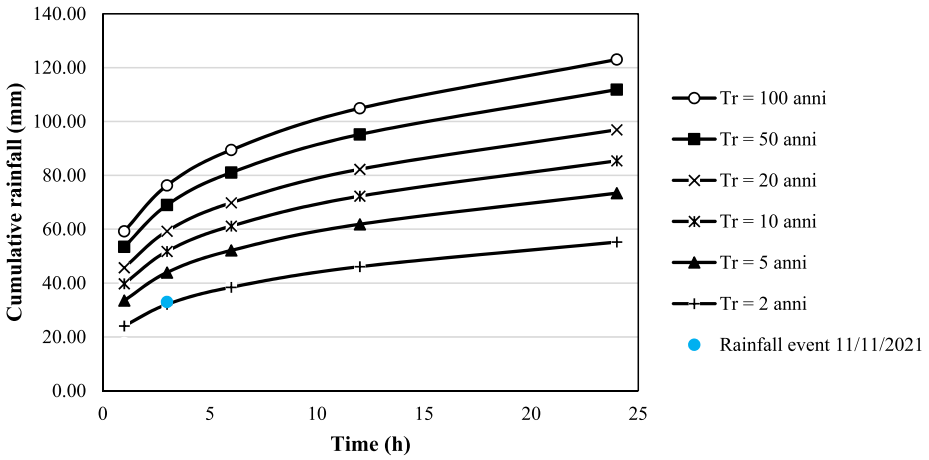

Fig. 5. Rainfall probability curves for different return periods of the Caltagirone pluviographic station (data by the Osservatorio delle Acque, 1928–2015) with the placement of the event occurred on 11th November 2021 (data by the SIAS, 2021).

Table 2
Spectral bands combination employed in the automatic supervised classification.

Spectral bands combination	Band number	Description	Central wavelengths (mm)	Spatial resolution (m)
True Color Image (TCI)	4	Visible Red	664.99	10
	3	Visible Green	559.0	10
	2	Visible Blue	492.1	10
Near-Infrared, Green and Blue (NGB)	8	Near-Infrared	832.9	10
	3	Visible Green	559.0	10
	2	Visible Blue	492.1	10
Vegetation Red Edge (VRE)	5	Red Edge	703.8	20
	6	Red Edge	739.1	20
	7	Red Edge	779.7	20

2.2.1. *Input dataset*

In this study Sentinel-2 images were used to perform the automatic supervised classification, since are free, full and open data accessible to all users with a high spatial resolution and a high revisit frequency. The Sentinel-2 mission allows to measure the Earth's reflected radiance in 13 spectral bands in the range of Visible (VIS), Near Infrared (NIR) and Short Wave Infrared (SWIR), with a variable spatial resolution from 10 to 60 m according to the different bands. In this work, the remote sensed images were employed with the original spatial resolution (10 m for VIS and NIR, 20 m for VRE) without applying any downscaling method. Moreover, the use of Level 2A images was preferred because they are already atmospherically corrected in contrast to Level 1C images. The decision to use this product type is also related to the consideration that its bands are more appropriate for vegetation analysis, due to its wavelength sensibility to the chlorophyll content and the phenological state, in addition to its better spatial resolution in comparison with other satellite images (Chaves et al., 2020; Praticò et al., 2021; Sánchez-Espinosa & Schröder, 2019).

2.2.2. *Classification process*

Free data from Sentinel missions (https://sentinel.esa.int/web/sentinel/home) were used in GIS environment to carry out supervised pixel-based classification of land cover based on the employ of different compositions images, in order to identify the best input image that allow to reach the highest accuracy. Since, in this study, were utilized satellite images with 10–20 m spatial resolution, a pixel-based approach is recommended rather than an object-based one, given that the size of the detected object is smaller than the pixel resolution (Praticò et al., 2021). The pixel-based approach is a spectral method that analyses the spectral information of each pixel with the aim of identifying the objects within images (Arcidiacono & Porto, 2012). For this purpose, based on physical proprieties, it is necessary to distinguish the information contained in the satellite images into classes or categories, in such a way that the degree of similarity is high between elements belonging to the same category and low between elements belonging to different categories. Taking into account the characteristics of the study area other six land cover classes to perform the classification, in addition to GR, were defined. The additional land cover classes were citrus orchards (CO), non-irrigated arable land (NAL), wood vegetation (WV), water (Wa), bare soil (BS) and greenhouses (Gh). Hence, the supervised classification allowed to classify pixels of unknown identity on the basis of areas with a known land use, called training areas (Bogoliubova & Tymków, 2014; Enderle & Weih, 2005).

Fig. 6 shows a summary of the methodology followed in the study. In brief, the methodological approach proposed consisted of three main steps: (i) a training phase, to select carefully a representative homogeneous set of pixel for each thematic class, called Area of Interest (AOIs), whose numerical information is processed in order to extract a unique spectral signature for each categories; (ii) an assignment phase, to employ the decision rule developed in the previous phase, by means of a classification algorithm, to associate a label of the thematic classes to all the pixels in the image; (iii) a validation phase, to evaluate the accuracy of the resultant thematic map, through the comparison between the labels assigned to the pixels during the classification process and a set of validation pixels, named as ground truth.

Once land cover classes were identified in the study area, it was necessary to select, for each of them, a certain number of AOIs, also called training pixels. The greater the number of AOIs picked for each category, the more typical is the spectral signature as capable of grasping the intrinsic variability to each of them. The set of spectral signatures obtained represent the training sample, necessary to make the classifier able to recognize the objects characterized by the same spectral response of the detected AOIs and to associate them with the correct thematic class. According to Ma et al. (2015) and Praticò et al. (2021) the final classification result is affected by the choice of training pixels, closely related to those of validation pixels, that is one of the highly crucial steps in the whole process. In truth, a conventional method to select training and validation pixels does not exist, but commonly the ratio between them is 70/30 (Gudiyangada Nachappa et al., 2020; Tsangaratos & Ilia, 2016). The validation pixels were defined by using

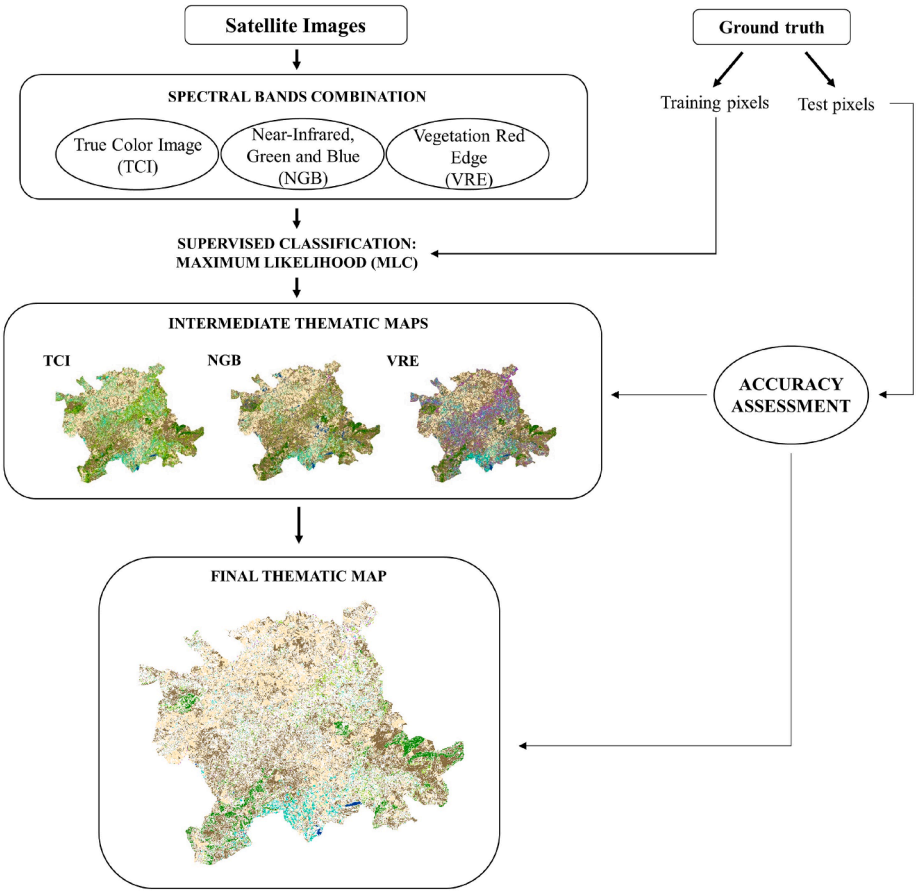

Fig. 6. Workflow applied for performing the automatic supervised classification by using Sentinel-2 images in a Geographic Information System (GIS) environment.

photointerpretation based on satellite images of Google Earth (https://www.google.com/earth/) and ground-based observations. The observation points of known coordinates detected directly at the field were selected according to the seven thematic classes previously defined, in order to improve their spectral signatures typicality. A total number of 2,304 pixels were surveyed; about 70 % of them (1,622 pixels) was selected as training pixels and about 30 % (682 pixels) was used as validation pixels. As soon as the classifier was trained, the supervised classification was launched. A statistical based classification algorithm, named as Maximum Likelihood (MLC), was employed to associate a label of the defined thematic classes to all the pixels in the image. During the classification process, the classifier performs a comparison between the statistical value of each pixels and each informational class, in order to assign every pixel to a specific thematic class for which the statistical distance, measured as mean and covariance, is less (Sisodia et al., 2014). Therefore, the smaller the statistical distance, the greater is the probability of pixel belonging to a category. MLC is based on Bayesian decision rule (Sisodia et al., 2014), which can be expressed as follows (Equation (1)):

$$P(v|C_i) = (2\pi)^{-\frac{N}{2}}|Y_i|^{-\frac{1}{2}}exp\left\{-\frac{1}{2}(v-Z_i)^T\right\}Y_i^{-1}(v-Z_i) \quad (1)$$

where $P(v|C_i)$ denotes the probability of finding a particular pixel at position v in each of the classes C_i, Z_i is the mean vector and Y_i is the covariance matrix of the data class in C_i.

The final product of this step was a thematic map containing the information related to all thematic classes. The described classification process was repeated for the three different combinations of spectral bands previously defined.

2.2.3. Statistical assessment

For each final product of the classification process an accuracy assessment procedure to analyses the quality of the thematic maps produced through the automatic supervised classification was performed. The error matrices related to each classification were implemented to represent maps accuracy, comparing information from validation points, known as ground truth, with information on classified images.

The confusion matrices were used to compute some accuracy measures (AMs) able to offer information about the quality of the classification: Overall Accuracy (OA), User's Accuracy (UA) and Producer's Accuracy (PA). According to Congalton & Green (2019) the OA (%) is the ratio between the number of correctly classified pixels (n_{ii}) and the total number of pixels included in the error matrix (n) (Eq. (2)). In contrast to OA, the UA and PA concern to the classification accuracies of each thematic class. The UA is given by the ratio between the numbers of correctly classified (n_{ii}) and all classified pixels in a specific class (n_{i+}) (Eq. (3)), while the PA is obtained by dividing the number of correctly classified pixels (n_{jj}) and the number of validation pixels in a given class (n_{+j}) (Eq. (4)).

$$OA = \frac{\sum_{i=1}^{k} n_{ii}}{n} \quad (2)$$

$$UA = \frac{n_{ii}}{n_{i+}} \quad (3)$$

$$PA = \frac{n_{jj}}{n_{+j}} \quad (4)$$

Another measure of the classification accuracy, named as Kappa Coefficient of Agreement ($\widehat{K}$), was evaluated. Kappa values range

between 0 and 1, showing the highest agreement for values close to 0.75 and the lowest agreement for values close to 0.4. The following relation, elaborated by Bishop et al.(1975), was used to compute $\widehat{K}$ (Eq. (5)):

$$\widehat{K} = \frac{N\sum_{i=1}^{r} X_{ii} - \sum_{i=1}^{r} X_i X_{+i}}{N^2 - \sum_{i=1}^{r} X_{i+} X_{+i}} \quad (5)$$

where r is the number of rows and columns in error matrix, N is the total number of observation, X_{ii} is the total number of pixels present in the major diagonal and X_{i+} and X_{+i} are the marginal total of rows and of columns respectively.

Once the accuracy was evaluated, it was necessary to combine the classified images in order to improve the localization and the quantification accuracy of the GR class, considering as valid just the pixels classified in all three different combinations of spectral bands as GR. This was helpful to overcome one of the limit of the automatic supervised classification process that is to distinguish classes or categories characterized by a very similar spectral response, such as different types of vegetation. This depends not only on the types of land cover, but also on the acquisition period of the remote sensed images used during the classification process that, in this work, is related to summer season. As the acquisition period varies, the climatic conditions and consequently spectral responses of the objects under study vary. The quality of the obtained final thematic map was also evaluated through the accuracy assessment procedure.

2.3. By-products availability to feed anaerobic digester in the study area

Considering the flood hydraulic risks increase associated with the wide distribution of GR along the watercourses embankments in the Calatino area and the presence of the biogas plant, it was necessary to estimate the availability of by-products, essential for starting the AD process. A GIS-based spatial analysis was carried out to evaluate the available amount of by-products from the close agro-industrial companies to feed the biogas plant managed by the SIMBIOSI Consortium. Due to the strong economic impact for their removal and disposal, the possibility of reusing the agricultural, food and livestock waste for energy production provides an opportunity for the farmers to reduce the management costs and to participate in achieving environmental benefits. The criterion that allowed to discriminate the suppliers of by-products is the geographical proximity between producers and consumers, measured in kilometers, to promote the Short Food Supply Chain (SFSC) sustainability goals. To assess the numbers of the available agro-industrial companies and their by-products, the considered distance between producers and consumer (the SIMBIOSI consortium) was 70 km from the latter. Thereby, the potential supplier companies identified by the spatial analysis performed in a GIS environment were 17, located in 8 different municipalities.

These farms are capable of providing plant and animal wastes to produce biogas by the AD process, belonging to the categories defined by the decree of 13 October 2016, n. 264, Annex 1 (Repubblica Italiana, 2016). Considering the surface area available for each agro-industrial companies, the output by-products typology and their average annual yield, the annual average availability of each of them was computed. The plant and animal wastes were split into three different categories: (i) animal by-products, which includes serum and poultry manure; (ii) agricultural by-products, involving vegetation mowing, full-field vegetables, artichokes, pulses and other vegetables; (iii) food and agro-industrial by-products, comprising pastazzo, pomace, orange, clementine, mandarin, lemons, satsuma, grapefruit, kaki, kiwi, pear, pomegranate, prickly pear, table grape, apricot, peaches, percoche peaches, plum, melons, avocado, mango, full-field vegetables, greenhouse vegetables (tomato, peels tomato, topinambur, garlic), pulses, artichokes. Specifically, the amount of by-products for each category is 12,000 tons/year of animal by-products, 93 tons/year of agricultural by-products and 30,796 tons/year of food and agro-industrial by-products.

In Fig. 7 is shown the overall picture related to the presence of agricultural, food and livestock industries, with a geographical proximity within the 70 km from the SIMBIOSI Consortium, that could provide plant and animal waste to supply the biogas plant located in the study area.

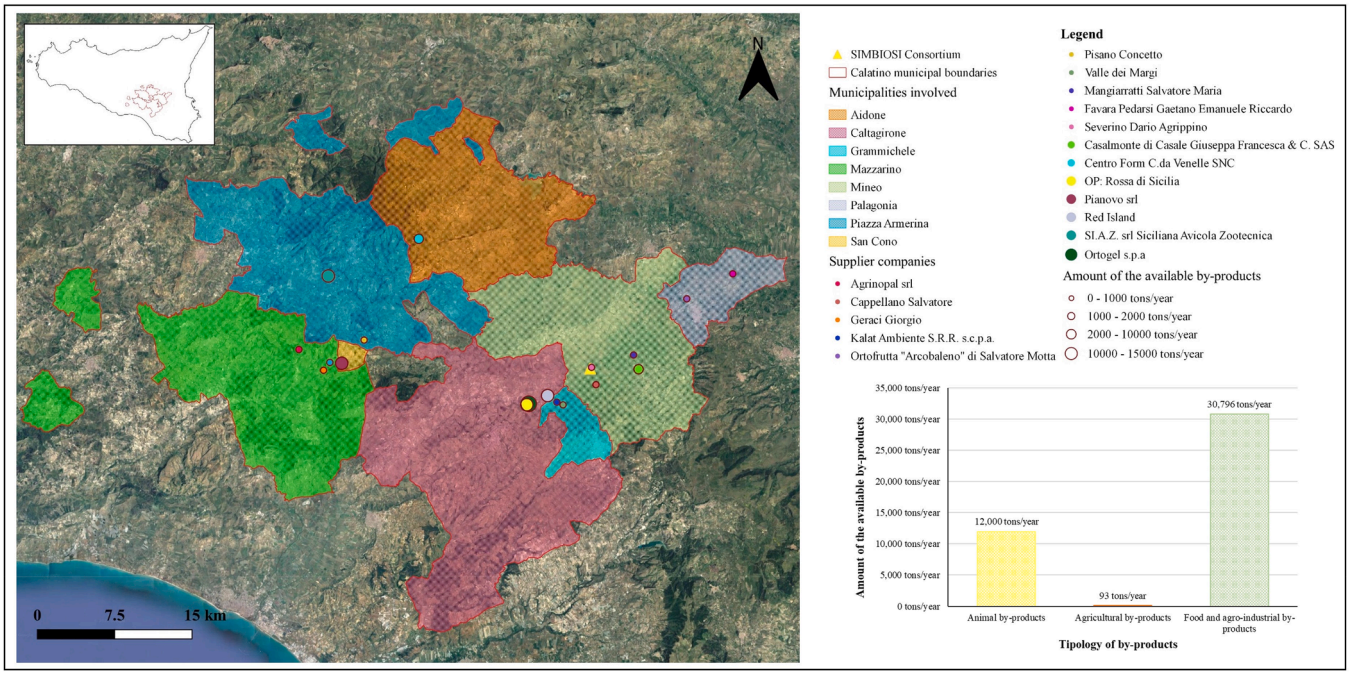

Fig. 7. Locations of potential supplier companies that could provide the necessary by-products to feed the biogas plant manage by SIMBIOSI Consortium. The columns chart contains the typology and amount of the available by-products for each firm.

Table 3
Confusion matrices and accuracy values for each adopted combination of spectral bands, according to the considered land cover classes: (A) TCI, (B) NGB, and (C) VRE.

A		Reference Data							∑	User's accuracy
		GR	NAL	CO	Wa	WV	BS	Gh		
Classified Data	Giant Reed (GR)	**27 %**	0 %	19 %	0 %	5 %	0 %	3 %	7 %	44 %
	Non-irrigated Arable Land (NAL)	20 %	**93 %**	8 %	15 %	5 %	17 %	26 %	30 %	60 %
	Citrus Orchards (CO)	33 %	2 %	**57 %**	5 %	17 %	2 %	5 %	17 %	49 %
	Water (Wa)	0 %	0 %	0 %	**55 %**	1 %	0 %	1 %	2 %	85 %
	Wood Vegetation (WV)	0 %	0 %	6 %	0 %	**61 %**	1 %	0 %	12 %	91 %
	Bare Soil (BS)	15 %	5 %	6 %	5 %	7 %	**78 %**	4 %	20 %	72 %
	Greenhouses (Gh)	5 %	0 %	4 %	20 %	4 %	2 %	**61 %**	12 %	76 %
	∑	12 %	19 %	15 %	3 %	18 %	18 %	15 %	100 %	
	Producer's accuracy	27 %	93 %	57 %	55 %	61 %	78 %	61 %		
						Overall accuracy:			65.63 %	
						Kappa Coefficient:			0.59	

B		Reference Data							∑	User's accuracy
		GR	NAL	CO	Wa	WV	BS	Gh		
Classified Data	Giant Reed (GR)	**37%**	0%	22%	0%	3%	0%	2%	9%	52%
	Non-irrigated Arable Land (NAL)	17%	**93%**	4%	20%	6%	17%	23%	29%	62%
	Citrus Orchards (CO)	20%	1%	**52%**	0%	15%	3%	6%	14%	54%
	Water (Wa)	0%	1%	0%	**65%**	0%	2%	1%	3%	76%
	Wood Vegetation (WV)	0%	0%	3%	0%	**69%**	2%	0%	13%	94%
	Bare Soil (BS)	22%	5%	18%	15%	7%	**76%**	5%	23%	62%
	Greenhouses (Gh)	4%	0%	1%	0%	1%	1%	**63%**	10%	91%
	∑	12%	19%	15%	3%	18%	18%	15%	100%	
	Producer's accuracy	37%	93%	52%	65%	69%	76%	63%		
						Overall accuracy:			67.55%	
						Kappa Coefficient:			0.61	

C		Reference Data							∑	User's accuracy
		GR	NAL	CO	Wa	WV	BS	Gh		
Classified Data	Giant Reed (GR)	**49%**	1%	27%	5%	4%	2%	10%	13%	47%
	Non-irrigated Arable Land (NAL)	6%	**83%**	1%	10%	2%	10%	8%	21%	77%
	Citrus Orchards (CO)	16%	0%	**53%**	0%	16%	2%	3%	13%	59%
	Water (Wa)	0%	0%	0%	**60%**	0%	1%	1%	2%	86%
	Wood Vegetation (WV)	0%	0%	4%	5%	**67%**	1%	0%	13%	93%
	Bare Soil (BS)	19%	13%	14%	20%	5%	**84%**	7%	25%	63%
	Greenhouses (Gh)	10%	3%	1%	0%	6%	1%	**71%**	14%	77%
	∑	12%	19%	15%	3%	18%	18%	15%	100%	
	Producer's accuracy	49%	83%	53%	60%	67%	84%	71%		
						Overall accuracy:			69.47%	
						Kappa Coefficient:			0.63	

3. Results

3.1. Identification of Arundo donax L. in the territory

Table 3 shows the main results obtained after the accuracy assessment procedure for each adopted combination of spectral bands during the automatic supervised classification process. The highest accuracy values were achieved using as input image the VRE composition, with an OA of 69.47 %, $\widehat{K}$ of 0.63, UA_{mean} of 71.59 % and PA_{mean} of 66.81 %. Also the NGB image, though less, allowed to attain good results, with an OA of 67.55 %, $\widehat{K}$ of 0.61, UA_{mean} of 68.25 % and PA_{mean} of 61.87 %. The worst performance was obtained when the classification was carried out on the TCI combination, with an OA of 65.63 %, $\widehat{K}$ of 0.59, UA_{mean} of 70.00 % and PA_{mean} of 65.00 %. Considering the results reached for each land cover class, it appears that the vegetation was better detected by means of a multispectral image that includes a spectral channel in the near infrared (NIR), due to a higher reflectivity of vegetated surfaces than in other spectral bands (Aqeel et al., 2011). In particular, according to the research objectives, the GR class was finer mapped by using both the NGB composition, with an UA of 51.72 % and PA of 37.04 %, and the VRE composition, with an UA of 46.51 % and PA of 49.38 %. As expected, the lowest accuracy values were attained using as input image the TCI combination, with an UA of 44.00 % and PA of 27.16 %.

Once the classification was performed and the accuracy was evaluated on the three different combinations of spectral bands, in order to obtain a more accurate localization and quantification of GR, a combination between the classified images was carried out (Fig. 8).

The procedure allowed to extract a thematic map containing for each informational class just the pixels common to the three classified images, with an OA of 85.02 %, $\widehat{K}$ of 0.81, UA_{mean} of 85.26 % and PA_{mean} of 79.06 % (Table 4). The results obtained after the accuracy assessment showed that thematic classes provided with a really different spectral response (like Gh, Wa, WV, BS and NAL) were classified with higher precision than other categories (like GR and CO) having a similar spectral response to other classes. As expected, it appears that often GR class was mixed up with other classes such as CO, NAL and BS reaching an UA of 76.47 % and PA of 46.43 %. Similarly, the CO class, though less, was frequently confused with the GR, WV and BS classes, achieving an UA of 68.18 % and PA of 75.00 %. The highest accuracy values were obtained when classifying Gh class, with an UA of 100.00 % and PA of 82.26 %, followed by WV class almost always correctly classified with an UA of 97.14 % and PA of 83.95 %. The remaining categories (NAL, Wa and BS) were detected with successful results reaching a values of UA ranged between 81.65 % and 91.67 % and values of PA varying between

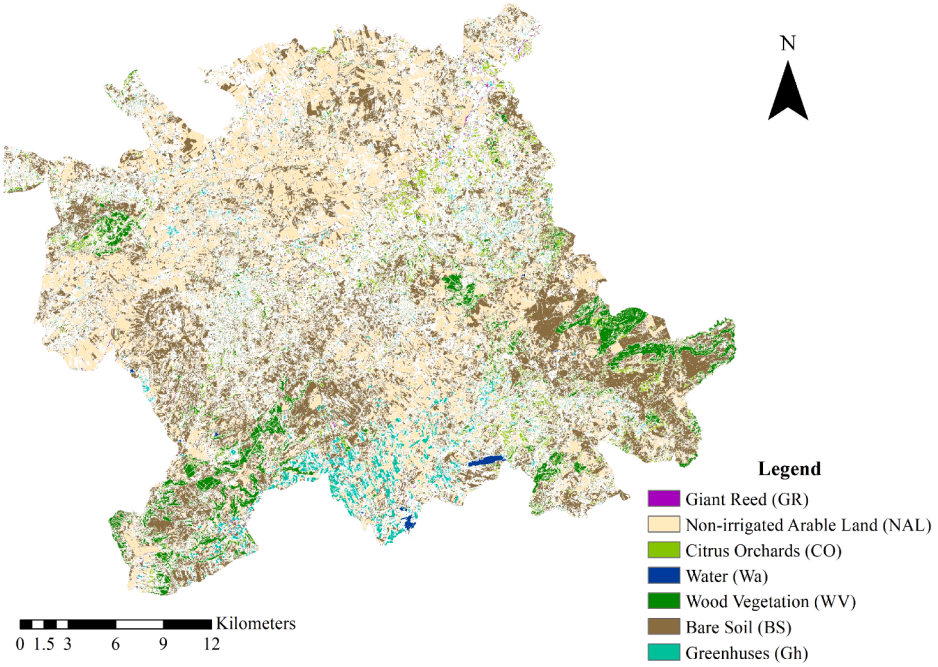

Fig. 8. Thematic map derived from the combination of the three classified images (TCI, NGB and VRE).

Table 4
Confusion matrix and accuracy values related to the thematic map derived from the combination of the three classified images (TCI, NGB and VRE), according to the considered land cover classes.

		Reference Data							∑	User's accuracy
		GR	NAL	CO	Wa	WV	BS	Gh		
Classified Data	Giant Reed (GR)	**46 %**	0 %	8 %	0 %	0 %	0 %	2 %	4 %	76 %
	Non-irrigated Arable Land (NAL)	18 %	**96 %**	3 %	14 %	2 %	9 %	8 %	30 %	82 %
	Citrus Orchards (CO)	14 %	0 %	**75 %**	0 %	10 %	0 %	3 %	10 %	68 %
	Water (Wa)	0 %	0 %	0 %	**79 %**	0 %	0 %	2 %	3 %	92 %
	Wood Vegetation (WV)	0 %	0 %	5 %	0 %	**84 %**	0 %	0 %	16 %	97 %
	Bare Soil (BS)	21 %	4 %	10 %	7 %	4 %	**91 %**	3 %	25 %	82 %
	Greenhouses (Gh)	0 %	0 %	0 %	0 %	0 %	0 %	**82 %**	12 %	100 %
	∑	6 %	26 %	9 %	3 %	19 %	23 %	14 %	100 %	
	Producer's accuracy	46 %	96 %	75 %	79 %	84 %	91 %	82 %		
						Overall accuracy:			85.02 %	
						Kappa Coefficient:			0.81	

78.57 % and 96.40 %.

Finally, the surface covered by GR in the study area (computed in GIS environment) was about 2 km^2. Considering an average biomass yield of about 5.89 kg/m^2, measured in open field conditions, and the spatial distribution previously assessed by the GIS-based analysis, the quantity of GR from the maintenance interventions of the watercourses embankments was estimated and would amount to about 11,780 tons $year^{-1}$.

4. Discussion

Several studies have reviewed the effects of riparian vegetation on channel geometry, bank stability and flow regimes finding a relationship between the type or density of vegetation and the river dynamics (Gran & Paola, 2001; Lama et al., 2021c; Lama and Cesare, 2022; Trimble, 2013; van de Lageweg et al., 2010). In recent times, Jourdain et al. (2018) claimed that the vegetation encroachment in fluvial environments can trigger an increase in flood risks due to a stream roughness rise which in turn leads to a flow velocity decrease and a water levels increase for given discharges. In particular, Coffman (2020) discussed about the invasive traits of GR describing it as one of the biggest threats to the riparian habitats in Mediterranean-type climate regions with flooding hydraulic risk increase. Also Spencer et al. (2013) highlighted the influence of riparian vegetation in channel water movement showing that especially the GR growth contributes to reduce mean water velocity by 46 % or 53 % and to increase the flooded area from 10 % to 19 %.

According to several authors, despite GR shows the traits of invasive plant species, including long canopy duration, rapid growth, high water use-efficiency and resistance to pests and diseases, all of these features are also requested for energy crops to produce biogas by AD (Barbagallo et al., 2014; Barney & DiTomaso, 2008; Corno et al., 2014; Crosti et al., 2010; Ge et al., 2016; Pilu et al., 2013). Numerous studies reported that the obtainable methane yield from GR with one single harvest is equal to 9580 Nm^3 CH_4 ha^{-1}, while with double harvest system biomethane production rises achieving values ranging from 11,585 to 12,981 Nm^3 CH_4 ha^{-1} (Antal, 2018; Corno et al., 2014; Ragaglini et al., 2014).

Considering that frequent riparian vegetation maintenance interventions are needed to reduce hydrogeological risk with considerably burden costs at the expense of public administration, several studies

discussed about the possibility of streamside vegetation reuse as biomass for energy production (Forzieri, 2012; Recchia et al., 2010; Rockwood et al., 2004).

Methods based on GIS were worldwide recognized as useful techniques to analyze biomasses availability for energy purpose, however a little number of studies utilize RS satellite data combined with GIS tools to identify riparian vegetation and to assess its availability for biogas and biomethane productions.

Concerning the classification process, the choice of testing different compositions of spectral bands, as input images, using the same set of reference data for training and validation, in order to investigate the influence on classification accuracy and to identify the most suitable input data for GR recognition, was in line with the finding of Praticò et al. (2021). Our results showed that applying the pixel-based MLC approach the final thematic map OA is generally high (85.02 %), compared to that obtained in other studies. For instance, Dillabaugh & King (2008) showed that the employment of Ikonos multispectral (4 m resolution) and panchromatic (1 m resolution) imagery to map riparian marshland composition and biomass, performing several MLC classification tests, lead to a significant accuracies from 61 % to 88 %. Also Forzieri et al. (2010) in his work observed that a pixel-based MLC approach, to identify and to monitor riparian vegetation, applied using data fusion of a QuickBird image and LIDAR data produced an encouraging accuracy with a very good level of agreement ($\widehat{K} = 0.77$). Similarly, Everitt et al. (2008) compared the use of QuickBird (2.4 m resolution) and SPOT 5 (10 m resolution) multispectral satellite imagery to map GR along the Rio Grande River by applying the MLC to classify the images. In this case study, results showed that both QuickBird and SPOT 5 satellite imagery can be used to recognize GR infestation with an OA of 83.2 % and 79.2 %, respectively. All of the studies discussed above claimed, in accordance with our study, that the MLC classification algorithm is a robust technique and allowed to achieve a high OA.

Furthermore, the results obtained highlighted, in line with previous finding, that adding the NIR band to the visible bands (Red, Green and Blue) the commission and omission errors decrease in favor of an increase in accuracy indicators (OA, PA and UA), thanks to the useful spectral information contained in this band and its high sensibility to chlorophyll content (Chaves et al., 2020; Praticò et al., 2021; Sánchez-Espinosa & Schröder, 2019). However, in order to improve the classification accuracy, other methods could be used. For instance, several studies reviewed by Yaseen (2021), applied successfully machine learning models for quality water bodies purposes, even combined with RS techniques.

Finally, this study showed that classifying species with very high spectral similarity can be lead to a misclassification errors with a low values of PA and UA affecting the classification results based on multispectral instead of hyperspectral images (Praticò et al., 2021; Somers & Asner, 2014). According to Everitt et al. (2005), Everitt et al. (2008), in fact, GR thematic class often was mixed up with other classes characterized with a very similar spectral response such as dry grass and scrub brush obtaining, in some cases, a lowest agreement level. In ours study, the combination of the classified images (TCI, NGB, VRE), considering as valid just the pixels classified in all three different combinations of spectral bands as GR, was helpful to improve the classification accuracy (PA of about 8.5 % and UA of about 28 %) of the GR class in terms of localization and quantification.

In general, despite the limit of the process, the pixel-based supervised classification allowed to detect GR with an acceptable accuracy value and to quantify its availability in the Calatino area for the biomethane production. As a consequence, the study could contribute to the achievement of the Sustainable Development Goals (SDGs), established by the United Nation Conference on Sustainable Development (Rio +20, 2012) as regard the management of water and energy resources. Especially, the results obtained and further analysis could be helpful to achieve goals 7th (Ensure access to affordable, reliable, sustainable and modern energy for all) and 11th (Make cities and human settlements inclusive, safe, resilient and sustainable), in order to reduce disaster risk associated with flooding and to increase the development of sustainable energy using biomass from the mowing of watercourses embankments.

5. Conclusion

The retrieval of riparian vegetation for energy purpose represents a sustainable way to recover management vegetation costs and to reduce some environmental impacts. Under this scenario, one of the biggest threats influencing the regular water movement in Mediterranean area watercourses is the presence of GR vegetation within stream channels. Nevertheless, due to its high biomass production and its being a no-food crop, not competing for land utilized for food supplies, GR could become a real opportunity to generate bioenergy. Several studies in literature have shown the GR capacity to reach much more biogas and biomethane productions per hectare than traditional energy crops.

In this study, a GIS-based methodology for the identification of GR spatial distribution was implemented, allowing to map GR with an acceptable accuracy value and to quantify its availability in the Calatino area for biogas and biomethane productions. Furthermore, the suitability of different combination of spectral bands, in terms of GR classification accuracy, was compared and evaluated. A bottleneck of this process is represented from the difficulty of the classifier to discriminate, in some cases, classes characterized by a very similar spectral response. The improvement of limited availability of RS data free and open to all user with a suitable resolution could be useful to overcame this limitation. However, RS technologies combined with GIS tools, thanks to their relative low revisiting time and high spatial resolution, could help responsible authorities to monitor riparian ecosystem dynamics and to mitigate the effects of natural hazards.

Finally, the duality of GR as an invasive hydrophyte plant and, at the same time, as an energy crop should be taken into consideration by public administrations to drive decision-making processes for a multifunctional maintenance of the riparian vegetation. To this end, this study could contribute to the development of vegetation management plans necessary to restore watercourses, reducing the risk of streams flooding in valley areas and at intersections with infrastructure works and getting new economic benefits at local scale.

CRediT authorship contribution statement

L. Sciuto: Writing – original draft, Writing – review & editing, Conceptualization, Methodology, Data curation, Software. **F. Licciardello:** Writing – review & editing, Conceptualization, Methodology, Data curation, Software. **A.C. Barbera:** Writing – review & editing, Conceptualization. **G. Cirelli:** Writing – review & editing, Conceptualization, Supervision.

Declaration of Competing Interest

The authors declare that they have no known competing financial interests or personal relationships that could have appeared to influence the work reported in this paper.

Data availability

Data will be made available on request.

Acknowledgements

The research was funded by the the International Doctorate in Agricultural, Food, and Environmental Science – Di3A – University of Catania. The authors thank the SIMBIOSI Consortium and its technical personnel for their availability and assistance during the field and laboratory activities. The work was carried out in the frame of the research

project “Strategie per migliorare l’efficienza d’uso dell’acqua per le colture mediterranee” (SaveIrriWater) Linea 2 Ricerca di Ateneo 2020-22 (Università degli Studi di Catania).

References

European Environment Agency. (2018). European waters — assessment of status and pres- sures 2018. *EEA Report No 7/2018*, https://www.eea.europa.eu/publications/state-of-wa.

Alavi-Borazjani, S.A., Capela, I., Tarelho, L.A.C., 2020. Over-acidification control strategies for enhanced biogas production from anaerobic digestion: A review. Biomass and Bioenergy 143 (June), 105833. https://doi.org/10.1016/j.biombioe.2020.105833.

Angelini, L.G., Ceccarini, L., Nassi o Di Nasso, N., Bonari, E., 2009. Comparison of Arundo donax L. and Miscanthus x giganteus in a long-term field experiment in Central Italy: Analysis of productive characteristics and energy balance. Biomass and Bioenergy 33 (4), 635–643.

Antal, G., 2018. Giant reed (Arundo donax L.) from ornamental plant to dedicated bioenergy species: review of economic prospects of biomass production and utilization. *International*. Journal of Horticultural Science 24 (1–2), 39–46. https://doi.org/10.31421/ijhs/24/1-2./1545.

Aqeel, M., Jamil, M., Yusoff, I., 2011. Biomass and Remote Sensing of Biomass. InTech.

Arcidiacono, C., Porto, S.M.C., 2012. Pixel-based classification of high-resolution satellite images for cropshelter coverage recognition. Acta Horticulturae 937 (September), 1003–1010. https://doi.org/10.17660/ActaHortic.2012.937.124.

Barbagallo, S., Barbera, A., Cirelli, G.L., Milani, M., Toscano, A., Albergo, R., 2013. Evaluation of herbaceous crops irrigated with treated wastewater for ethanol production. Journal of Agricultural Engineering 44 (2s), 554–559. https://doi.org/10.4081/jae.2013.s2.e110.

Barbagallo, S., Barbera, A.C., Cirelli, G.L., Milani, M., Toscano, A., 2014. Reuse of constructed wetland effluents for irrigation of energy crops. Water Science and Technology 70 (9), 1465–1472. https://doi.org/10.2166/wst.2014.383.

Barney, J.N., DiTomaso, J.M., 2008. Nonnative species and bioenergy: Are we cultivating the next invader? BioScience 58 (1), 64–70. https://doi.org/10.1641/B580111.

Bishop, Y., Fienberg, S., Holland, P., 1975. Discrete Multivariate Analysis — Theory and Practice. MIT Press, Cambridge, MA.

Bogoliubova, A., Tymków, P., 2014. Land cover changes and dynamics of Yuntolovsky reserve. Electronic Journal of Polish Agricultural Universities 17. http://www.ejpau.media.pl/volume17/issue3/art-03.html.

Borin, M., Barbera, A.C., Milani, M., Molari, G., Zimbone, S.M., Toscano, A., 2013. Biomass production and N balance of giant reed (Arundo donax L.) under high water and N input in Mediterranean environments. European Journal of Agronomy 51, 117–119. https://doi.org/10.1016/j.eja.2013.07.005.

Cai, J., Liu, R., Deng, C., 2008. An assessment of biomass resources availability in Shanghai: 2005 analysis. Renewable and Sustainable Energy Reviews 12 (7), 1997–2004. https://doi.org/10.1016/j.rser.2007.04.003.

Carvalho, L., Mackay, E.B., Cardoso, A.C., Baattrup-Pedersen, A., Birk, S., Blackstock, K. L., Borics, G., Borja, A., Feld, C.K., Ferreira, M.T., Globevnik, L., Grizzetti, B., Hendry, S., Hering, D., Kelly, M., Langaas, S., Meissner, K., Panagopoulos, Y., Penning, E., Rouillard, J., Sabater, S., Schmedtje, U., Spears, B.M., Venohr, M., van de Bund, W., Solheim, A.L., 2019. Protecting and restoring Europe’s waters: An analysis of the future development needs of the Water Framework Directive. Science of the Total Environment 658, 1228–1238.

Chaves, M.E.D., Picoli, M.C.A., Sanches, I.D., 2020. Recent applications of Landsat 8/OLI and Sentinel-2/MSI for land use and land cover mapping: A systematic review. Remote Sensing 12 (18). https://doi.org/10.3390/rs12183062.

G.C. Coffman Giant Reed (Arundo donax): Streams and Water Resources. Managing Water Resources and Hydrological Systems, October B.D. Fath S.E. Jørgensen M. Cole Managing Water Resources and Hydrological Systems 2 CRC Press 327 335.

Commission, E., 2017. Fitness Check (evaluation) of the Water Framework Directive (2000/60/EC) and the Floods Directive (2007/60/EC). Evaluation and fitness check roadmap. 5, 13.

European Commission. (2012). A blueprint to safeguard Europe’s water resources. Communication from the Commission to the European Parliament, the Council, the European Economic and Social Committee and the Committee of the Regions. *COM (2012) 673 Final*.

Congalton, R. G., & Green, K. (2019). *Assessing the accuracy of remotely sensed data: principles and practices*.

Corno, L., Pilu, R., Adani, F., 2014. Arundo donax L.: A non-food crop for bioenergy and bio-compound production. Biotechnology Advances 32 (8), 1535–1549. https://doi.org/10.1016/j.biotechadv.2014.10.006.

Crosti, R., Cascone, C., Cipollaro, S., 2010. Use of a weed risk assessment for the Mediterranean region of Central Italy to prevent loss of functionality and biodiversity in agro-ecosystems. Biological Invasions 12 (6), 1607–1616. https://doi.org/10.1007/s10530-009-9573-6.

Dillabaugh, K.A., King, D.J., 2008. Riparian marshland composition and biomass mapping using Ikonos imagery. Canadian Journal of Remote Sensing 34 (2), 143–158. https://doi.org/10.5589/m08-011.

Enderle, D.I., Weih, R.C.J., 2005. Integrating Supervised and Unsupervised Classification Methods to Develop a More Accurate Land Cover Classification. Journal of the Arkansas Academy of Science 59, 10. http://scholarworks.uark.edu/jaashttp://scholarworks.uark.edu/jaas/vol59/iss1/10.

Everitt, J.H., Yang, C., Deloach, C.J., 2005. Remote sensing of giant reed with QuickBird satellite imagery. Journal of Aquatic Plant Management 43 (JUL.), 81–85.

Everitt, J.H., Yang, C., Fletcher, R., Deloach, C.J., 2008. Comparison of QuickBird and SPOT 5 satellite imagery for mapping giant reed. Journal of Aquatic Plant Management 46 (1), 77–82.

Forzieri, G., 2012. Satellite retrieval of woody biomass for energetic reuse of riparian vegetation. Biomass and Bioenergy 36 (2), 432–438. https://doi.org/10.1016/j.biombioe.2011.10.036.

Forzieri, G., Moser, G., Vivoni, E.R., Castelli, F., Canovaro, F., 2010. Riparian Vegetation Mapping for Hydraulic Roughness Estimation Using Very High Resolution Remote Sensing Data Fusion. Journal of Hydraulic Engineering 136 (11), 855–867. https://doi.org/10.1061/(asce)hy.1943-7900.0000254.

Ge, X., Xu, F., Vasco-Correa, J., Li, Y., 2016. Giant reed: A competitive energy crop in comparison with miscanthus. Renewable and Sustainable Energy Reviews 54, 350–362. https://doi.org/10.1016/j.rser.2015.10.010.

Gran, K., Paola, C., 2001. Riparian vegetation controls on braided stream dynamics. Water Resources 37 (12), 3275–3283.

Gudiyangada Nachappa, T., Kienberger, S., Meena, S.R., Hölbling, D., Blaschke, T., 2020. Comparison and validation of per-pixel and object-based approaches for landslide susceptibility mapping. Geomatics, Natural Hazards and Risk 11 (1), 572–600. https://doi.org/10.1080/19475705.2020.1736190.

Italiana, R., 2016. Decreto 13 ottobre 2016, n. 264. Gazzetta Ufficiale 38, 15–36.

Jiménez-Ruiz, J., Hardion, L., Del Monte, J.P., Vila, B., Santín-Montanyá, M.I., 2021. Monographs on invasive plants in Europe N° 4: Arundo donax L. Botany Letters 168 (1), 131–151. https://doi.org/10.1080/23818107.2020.1864470.

Jourdain, C., Claude, N., Antoine, G., Tassi, P., Cordier, F., Paquier, A., Rivière, N., 2018. Influence of flood regime on riparian vegetation dynamics in rivers with alternate bars. E3S Web of Conferences 40, 02025.

Kumar Khanal, S., Lü, F., Wong, J.W.C., Wu, D.i., Oechsner, H., 2021. Anaerobic digestion beyond biogas. Bioresource Technology 337, 125378.

Kumar, A., Kumar, N., Baredar, P., Shukla, A., 2015. A review on biomass energy resources, potential, conversion and policy in India. Renewable and Sustainable Energy Reviews 45, 530–539. https://doi.org/10.1016/j.rser.2015.02.007.

Lama, Giuseppe Francesco Cesare, & Crimaldi, M. (2022). Remote Sensing of Ecohydrological, Ecohydraulic, and Ecohydrodynamic Phenomena in Vegetated Waterways: The Role of Leaf Area Index (LAI). *January*, 54. https://doi.org/10.3390/iecag2021-09728.

Lama, G.F.C., Errico, A., Pasquino, V., Mirzaei, S., Preti, F., Chirico, G.B., 2021a. Velocity uncertainty quantification based on Riparian vegetation indices in open channels colonized by Phragmites australis. Journal of Ecohydraulics 7 (1), 71–76. https://doi.org/10.1080/24705357.2021.1938255.

Lama, Giuseppe Francesco Cesare, Crimaldi, M., Pasquino, V., Padulano, R., & Chirico, G. B. (2021b). Bulk drag predictions of riparian arundo donax stands through UAV-acquired multispectral images. *Water (Switzerland)*, *13*(10), 1–19. https://doi.org/10.3390/w13101333.

Lama, G.F.C., Rillo Migliorini Giovannini, M., Errico, A., Mirzaei, S., Padulano, R., Chirico, G.B., Preti, F., 2021c. Hydraulic efficiency of green-blue flood control scenarios for vegetated rivers: 1D and 2D unsteady simulations. Water (Switzerland) 13 (19), 2620.

Li, J., Claude, N., Tassi, P., Cordier, F., Vargas-Luna, A., Crosato, A., Rodrigues, S., 2022. Effects of Vegetation Patch Patterns on Channel Morphology: A Numerical Study. Journal of Geophysical Research: Earth Surface 127 (5), 1–20. https://doi.org/10.1029/2021JF006529.

Lowe, S., Browne, M., Boudjelas, S., & De Poorter, M. (2000). 100 of the World’s Worst Invasive Alien Species A selection from the Global Invasive Species Database. *Published by The Invasive Species Specialist Group (ISSG) a Specialist Group of the Species Survival Commission (SSC) of the World Conservation Union (IUCN), 12pp. First Published as Special Lift-out in Aliens 12, December 2000. Updated and Reprinted Vers*.

Ma, L., Cheng, L., Li, M., Liu, Y., Ma, X., 2015. Training set size, scale, and features in Geographic Object-Based Image Analysis of very high resolution unmanned aerial vehicle imagery. ISPRS Journal of Photogrammetry and Remote Sensing 102, 14–27. https://doi.org/10.1016/j.isprsjprs.2014.12.026.

Mahmood, M.I., Elagib, N.A., Horn, F., Saad, S.A.G., 2017. Lessons learned from Khartoum flash flood impacts: An integrated assessment. Science of the Total Environment 601–602, 1031–1045. https://doi.org/10.1016/j.scitotenv.2017.05.260.

Mantineo, M., D’Agosta, G.M., Copani, V., Patanè, C., Cosentino, S.L., 2009. Biomass yield and energy balance of three perennial crops for energy use in the semi-arid Mediterranean environment. Field Crops Research 114 (2), 204–213. https://doi.org/10.1016/j.fcr.2009.07.020.

Meixner, H., Schnauder, I., Bölscher, J., & Iordache, V. (2006). *Heft 66 Hydraulic , Sedimentological and Ecological Problems of Multifunctional Riparian Forest Management – RIPFOR – Guidelines for End-Users* (Issue January).

Naiman, R. J., Decamps, H., & Pollock, M. (1993). The Role of Riparian Corridors in Maintaining Regional Biodiversity Author (s): Robert J . Naiman , Henri Decamps and Michael Pollock Published by : Ecological Society of America Stable URL : http://www.jstor.org/stable/1941822 . THE ROLE OF RIPARIAN CO. *Ecological Applications*, *3*(2), 209–212.

Pantaleo, A., Gennaro, B.D., Shah, N., 2013. Assessment of optimal size of anaerobic co-digestion plants: An application to cattle farms in the province of Bari (Italy). Renewable and Sustainable Energy Reviews 20, 57–70. https://doi.org/10.1016/j.rser.2012.11.068.

Pilu, R., Bucci, A., Badone, F.C., Landoni, M., 2012. Giant reed (Arundo donax L.): A weed plant or a promising energy crop? African Journal of Biotechnology 11 (38), 9163–9174. https://doi.org/10.5897/ajb11.4182.

Pilu, R., Manca, A., Landoni, M., 2013. Arundo donax as an energy crop: pros and cons of the utilization of this perennial plant. Maydica 58, 54–59.

Praticò, S., Solano, F., Di Fazio, S., Modica, G., 2021. Machine Learning Classification of Mediterranean Forest Habitats in Google Earth Engine Based on Seasonal Sentinel-2 Time-Series and Input Image Composition Optimisation. Remote Sensing 13 (4), 1–28. https://doi.org/10.3390/rs13040586.

Ragaglini, G., Dragoni, F., Simone, M., Bonari, E., 2014. Suitability of giant reed (Arundo donax L.) for anaerobic digestion: Effect of harvest time and frequency on the biomethane yield potential. Bioresource Technology 152, 107–115. https://doi.org/10.1016/j.biortech.2013.11.004.

Recchia, L., Cini, E., Corsi, S., 2010. Multicriteria analysis to evaluate the energetic reuse of riparian vegetation. Applied Energy 87 (1), 310–319. https://doi.org/10.1016/j.apenergy.2009.08.034.

Roberts, J.J., Cassula, A.M., Osvaldo Prado, P., Dias, R.A., Balestieri, J.A.P., 2015. Assessment of dry residual biomass potential for use as alternative energy source in the party of General Pueyrredón, Argentina. Renewable and Sustainable Energy Reviews 41, 568–583. https://doi.org/10.1016/j.rser.2014.08.066.

D.L. Rockwood C.V. Naidu D.R. Carter M. Rahmani T.A. Spriggs C. Lin G.R. Alker J.G. Isebrands S.A. Segrest Short-rotation woody crops and phytoremediation: Opportunities for agroforestry? 2004 10.1007/978-94-017-2424-1_4 51 63.

Sánchez-Espinosa, A., Schröder, C., 2019. Land use and land cover mapping in wetlands one step closer to the ground: Sentinel-2 versus landsat 8. Journal of Environmental Management 247 (May), 484–498. https://doi.org/10.1016/j.jenvman.2019.06.084.

Shanmugapriya, P., Rathika, S., Ramesh, T., Janaki, P., 2019. Applications of Remote Sensing in Agriculture – A Review. International Journal of Current Microbiology and Applied Sciences 8 (01), 2270–2283. https://doi.org/10.20546/ijcmas.2019.801.238.

Sisodia, P.S., Tiwari, V., Kumar, A., 2014. Analysis of Supervised Maximum Likelihood Classification for remote sensing image. International Conference on Recent Advances and Innovations in Engineering, ICRAIE 2014, 14–17. https://doi.org/10.1109/ICRAIE.2014.6909319.

Somers, B., Asner, G.P., 2014. Tree species mapping in tropical forests using multi-temporal imaging spectroscopy: Wavelength adaptive spectral mixture analysis. International Journal of Applied Earth Observation and Geoinformation 31 (1), 57–66. https://doi.org/10.1016/j.jag.2014.02.006.

Spencer, D.F., Colby, L., Norris, G.R., 2013. An evaluation of flooding risks associated with giant reed (Arundo donax). Journal of Freshwater Ecology 28 (3), 397–409. https://doi.org/10.1080/02705060.2013.769467.

Todo, K., Sato, K., 2002. Directive 2000/60/EC of the European Parliament and of the Council of 23 October 2000 establishing a framework for Community action in the field of water policy. Environmental Research Quarterly 66–106.

Trimble, S.W., 2013. Effects of Riparian Vegetation on Stream Channel Stability and Sediment Budgets. Riparian Vegetation and Fluvial Geomorphology 153–169. https://doi.org/10.1029/008WSA12.

Tsangaratos, P., Ilia, I., 2016. Comparison of a logistic regression and Naïve Bayes classifier in landslide susceptibility assessments: The influence of models complexity and training dataset size. Catena 145, 164–179. https://doi.org/10.1016/j.catena.2016.06.004.

Valenti, F., Porto, S.M.C., Dale, B.E., Liao, W., 2018a. Spatial analysis of feedstock supply and logistics to establish regional biogas power generation: A case study in the region of Sicily. Renewable and Sustainable Energy Reviews 97 (August), 50–63. https://doi.org/10.1016/j.rser.2018.08.022.

Valenti, F., Porto, S.M.C., Selvaggi, R., Pecorino, B., 2018b. Evaluation of biomethane potential from by-products and agricultural residues co-digestion in southern Italy. Journal of Environmental Management 223 (June), 834–840. https://doi.org/10.1016/j.jenvman.2018.06.098.

van de Lageweg, W. I., van Dijk, W. M., Hoendervoogt, R., & G., K. M. (2010). *Effects of riparian vegetation on experimental channel dynamics*. 1331–1338.

Yanli, Y., Peidong, Z., Wenlong, Z., Yongsheng, T., Yonghong, Z., Lisheng, W., 2010. Quantitative appraisal and potential analysis for primary biomass resources for energy utilization in China. Renewable and Sustainable Energy Reviews 14 (9), 3050–3058. https://doi.org/10.1016/j.rser.2010.07.054.

Yaseen, Z.M., 2021. An insight into machine learning models era in simulating soil, water bodies and adsorption heavy metals: Review, challenges and solutions. Chemosphere 277, 130126. https://doi.org/10.1016/j.chemosphere.2021.130126.